Thermal Resistance Models for Non-Circular Moving Heat Sources on a Half Space

Y. S. Muzychka
Assistant Professor
Faculty of Engineering and Applied Science,
Memorial University of Newfoundland,
St.John's, NF, Canada, A1B 3X5
e-mail: yuri@engr.mun.ca

M. M. Yovanovich
Distinguished Professor Emeritus
Fellow ASME
Department of Mechanical Engineering
University of Waterloo
Waterloo, ON, Canada, N2L 3G1
e-mail: mmyov@mhtl.uwaterloo.ca

Solutions to stationary and moving heat sources on a half space are reviewed for rectangular and elliptic contacts. The effects of shape, heat flux distribution, and orientation with respect to the direction of motion are examined. The dimensionless thermal resistance is shown to be a weak function of heat source shape if the square root of contact area is used as a characteristic length scale. Simple expressions are developed for calculating total thermal resistances of non-circular moving heat sources by combining asymptotic solutions for large and small values of the Peclet number. Both uniform and parabolic heat flux distributions are examined. A model is developed for predicting average or maximum flash temperatures of real sliding contacts. Comparisons of the proposed model are made with numerical solutions for two cases involving non-circular contacts. [DOI: 10.1115/1.1370516]

Keywords: Conduction, Contact Resistance, Heat Transfer, Modeling, Tribology

Introduction

The analysis of heat transfer from sliding and rolling contacts is important in many tribological applications such as ball bearing and gear design. In these applications heavily loaded contacts are typical and knowledge of the contact temperatures which result from frictional heat generation is required for minimizing thermal related problems such as scoring, lubricant breakdown, and adhesive wear due to flash welding.

A review of typical tribology books such as the texts by Halling [1] and Williams [2], and Handbook sections by Winer and Cheng [3] and Cowan and Winer [4] shows that the analysis of heat transfer from sliding or rolling contacts has not been extensively modelled. These reviews generally present equations and results for only one configuration, the circular contact. Although this contact geometry arises quite frequently in tribology applications, others such as the elliptic contact are also quite common in ball bearing and gear applications where non-conforming contacts prevail [5–7].

The analysis for moving heat sources which is presented in a number of tribology references [1–4], is based upon the assumption that one of the contacts can be modelled as a stationary heat source and the other as a fast moving heat source. In many problems the assumption of a fast moving heat source may not be valid and the analysis will incorrectly predict the average or maximum contact temperature. With this in mind, Tian and Kennedy [8] developed accurate correlations for the circular and square heat source which predict the temperature for any speed. These correlations were then used to formulate models for predicting flash temperatures in sliding asperities.

In a recent paper [9], a hybrid computational method for non-circular heat sources was developed. For this method, a numerical approach based upon the superposition of point heat sources was employed for the stationary portion and a transient finite element method was employed for the moving portion. This new approach was then used to predict temperatures in a steel/bronze sliding contact problem, with sliding motion normal and parallel to the grinding direction. The primary motivation for the work of Neder et al. [9] was that the conventional approach adopted in most tribology references was not applicable to non-circular heat sources.

The present work discusses various aspects of heat transfer in tribological applications involving stationary and sliding contacts. In all cases heat is either supplied to the contact or is generated through contact friction. This paper has four objectives. These are (i) provide a comprehensive review of the literature related to stationary and moving heat sources on half space, (ii) examine the effect that heat source shape and heat flux distribution have on the thermal resistance, (iii) develop a model which is applicable to a heat source of arbitrary shape and flux distribution, and (iv) use the proposed model to predict the flash temperature in a non-circular contact for real surfaces. In addressing these issues, a number of gaps in the literature have been filled. In addition, a clear and consistent approach to modeling arbitrary contacts has been developed. Presently, the field of tribology has only adopted a simplified approach in the prediction of contact temperatures due to sliding. The present approach does not allow for the effect of shape, aspect ratio, and flux distribution to be modelled easily. This was the primary motivation of the development of a hybrid numerical scheme by Neder et al. [9]. The expressions and method developed in the present work have been validated against a small set of numerical data for real and ideal contacts. The results of Neder et al. [9] are readily computed using the present approach with significantly less effort.

Governing Equations

A review of the literature [3,4,8,10–15], reveals that extensive analysis of the problem has been undertaken for various contact spot shapes and thermal boundary conditions for both stationary and moving heat sources.

The governing equation for a moving heat source may be obtained from the transient heat conduction equation with a transformation of variables [13]. The resulting equation for steady state conditions, is

$$\frac{\partial^2 T}{\partial x^2}+\frac{\partial^2 T}{\partial y^2}+\frac{\partial^2 T}{\partial z^2}=\frac{V}{\alpha}\frac{\partial T}{\partial x}, \tag{1}$$

where the coordinate system is fixed to the heat source and the half space moves beneath it with velocity V, see Figs. 1 and 2.

Contributed by the Heat Transfer Division for publication in the JOURNAL OF HEAT TRANSFER. Manuscript received by the Heat Transfer Division April 24, 2000; revision received January 8, 2001. Associate Editor: A. Bejan.

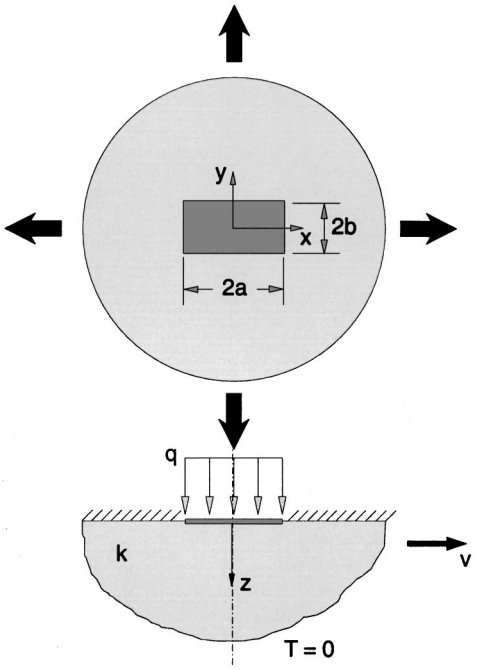

Fig. 1 Rectangular heat source

The thermal boundary conditions are constant or zero temperature in regions remote from the source, i.e., $r=\sqrt{x^2+y^2+z^2}\rightarrow\infty$, $T\rightarrow T_b$, or $T(x\rightarrow\pm\infty, y\rightarrow\pm\infty, z\rightarrow\infty)=T_b=0$ and prescribed heat flux q over the source area $\partial T/\partial z|_{z=0}=-q(x,y)/k$ while the region outside of the source area is assumed to be adiabatic $\partial T/\partial z|_{z=0}=0$.

Solution to Eq. (1) is usually obtained by superposition of the point heat source [11]

$$T-T_b=\left(\frac{Q}{2\pi kr}\right)e^{-V/2\alpha(r-x)} \tag{2}$$

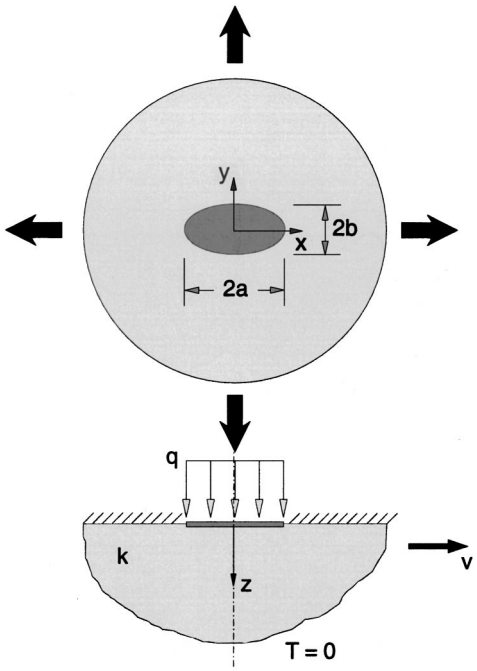

Fig. 2 Elliptic heat source

over the region of contact, where $r=\sqrt{x^2+y^2+z^2}$. Solution of the moving heat source by means of Eq. (2) is rather involved, requiring numerical integration. Solutions for the square and circular contact are tabulated in Tian and Kennedy [8]. A simpler approach based upon the combination of asymptotic solutions is presented in a later section for the arbitrarily shaped heat source.

Asymptotic Solutions

Stationary Heat Sources. If the velocity of the heat source is small $(V/\alpha\rightarrow 0)$, the governing equation reduces to Laplace's equation

$$\frac{\partial^2 T}{\partial x^2}+\frac{\partial^2 T}{\partial y^2}+\frac{\partial^2 T}{\partial z^2}=0 \tag{3}$$

with the same boundary conditions prescribed earlier.

Many solutions for stationary heat source problems have been obtained by superposition of the point heat source [11] on a half space

$$T-T_b=\frac{Q}{2\pi kr}, \tag{4}$$

where $r=\sqrt{x^2+y^2+z^2}$. Solutions for various heat flux distributions and source shapes have been found [14–16]. Of particular interest are the solutions for the rectangular and elliptical heat sources which contain the limiting cases for the square and circular contacts.

Moving Heat Sources. If the velocity of the heat source is large $(V/\alpha\rightarrow\infty)$, Eq. (1) simplifies to give

$$\frac{\partial^2 T}{\partial z^2}=\frac{V}{\alpha}\frac{\partial T}{\partial x}. \tag{5}$$

Equation (5) is essentially the one dimensional diffusion equation for a half-space with $t=x/V$. This equation assumes that heat conduction into the half space is one-dimensional and the solution may be approximated by the equation for heat flow at the surface of a half space with flux specified boundary conditions [11,12]

$$T-T_b=\frac{2q}{k\sqrt{\pi}}\sqrt{\alpha t}, \tag{6}$$

where t must be replaced by the effective traverse time $t=2x'/V$, and x' is the distance from an arbitrary point within the source to the leading edge of the source.

This approach was applied by Jaeger [12] for the strip and square heat sources, by Archard [17] for the circular source for the uniform heat flux distribution, and by Francis [18] for the circular heat source having a parabolic heat flux distribution. Later, it will be applied to obtain a solution for an elliptical heat source and comparisons will be made with the solution of Jaeger [12] for a rectangular source.

No solution was found for the equivalent isothermal moving heat source for a circular contact. A solution for this boundary condition may be obtained by extending the work of Francis [18] or Tian and Kennedy [8] for the parabolic heat flux distribution. The solution for a moving elliptic heat source with uniform and parabolic heat flux distribution will be obtained in a later section.

The analysis based on Eq. (6) is only valid for large values of the dimensionless group $\mathrm{Pe}=Va/\alpha$, or Peclet number. This group may be interpreted as a measure of the relative thermal penetration depth, δ/a, of heat into the half space. Beginning with the definition, $\delta=\sqrt{\pi\alpha t}$, which is the thermal penetration depth for heat flow into a half space, the relative penetration depth for a circular contact is

$$\frac{\delta}{a}\sim\frac{\sqrt{\pi\alpha t}}{a}. \tag{7}$$

If the traverse time for a moving circular heat source is taken to be $t=2a/V$, then Eq. (7) may be written as

$$\frac{\delta}{a}\sim\sqrt{\frac{2\pi\alpha}{Va}}\sim\frac{\sqrt{2\pi}}{\sqrt{\mathrm{Pe}}}. \tag{8}$$

Thus if $\mathrm{Pe}\to\infty$, the penetration δ is small, and may be taken to be one-dimensional since the spreading of heat into the half-space is negligible. On the other hand, if $\mathrm{Pe}\to 0$, the spreading of heat into the substrate will be significant. A solution for all values of Peclet number can only be obtained numerically.

Review and Solution of Stationary and Moving Heat Sources

A discussion of a number of important solutions for sliding heat sources is now presented. In many cases, gaps existed in the literature, and the present authors have developed new solutions for a number of problems. These are discussed throughout the sections that follow.

Stationary Heat Sources (Pe→0). Extensive analysis of heat conduction from isolated heat sources on a half space has been performed by a number of researchers [11,14–16,19]. The simplest contact geometry is the circular contact. The analysis has been performed for three heat flux distributions: the uniform heat flux, parabolic heat flux, and the inverse parabolic heat flux. The inverse parabolic heat flux represents a uniform temperature distribution over the contact area. The solutions for the dimensionless thermal resistance for these three cases are summarized in Table 1.

The thermal resistance may be defined with respect to the average surface temperature such that

$$\overline{R}=\frac{\overline{T}_c-T_b}{Q} \tag{9}$$

or with respect to the maximum surface temperature such that

$$\hat{R}=\frac{\hat{T}_c-T_b}{Q}. \tag{10}$$

A dimensionless thermal resistance may be defined as

$$R^*=Rk\mathcal{L}, \tag{11}$$

where $\mathcal{L}$ is an appropriate characteristic length related to the heat source area [5,6,14–16]. This thermal resistance is a spreading resistance due to the transfer of heat through a finite discrete point of contact. Spreading resistance concepts appear in any analysis of stationary or sliding contact problems in heat transfer and tribology, and form the basis for the field of thermal contact conductance.

In most tribological applications involving frictional heat generation, the average heat flux $\overline{q}=Q/A$ is known. What may not be known precisely, is the distribution of heat flux $q(x,y)$ over the contact. If the contact is Hertzian, the distribution of frictional heat generation may be represented by Case C in Table 1 [15]. In most analyses the assumption of a uniform heat flux distribution is often made. The effect of heat flux distribution on the thermal resistance based upon the average contact temperature is small. The variation from the uniform flux distribution is −7.4 percent for the isothermal heat source and +4.1 percent for the parabolic heat source. Thus the uniform heat flux distribution may be taken as representative of the mean value if the exact flux distribution is not known. If the resistance is based upon the maximum source temperature, the variation from the uniform flux distribution is −21.4 percent for the isothermal heat source and +17.9 percent for the parabolic heat source. In both cases the maximum and minimum values for the average or maximum source temperature are bounded by the solutions for Case A and Case C.

Table 1 Effect of boundary conditions on stationary circular heat source [15]

Case	Flux Distribution	$\overline{R}ka$	$\hat{R}ka$
A - Isothermal	$\frac{1}{2}\overline{q}\frac{1}{\sqrt{1-(r/a)^2}}$	$\frac{1}{4}=0.250$	$\frac{1}{4}=0.250$
B - Isoflux	$\overline{q}$	$\frac{8}{3\pi^2}\approx 0.270$	$\frac{1}{\pi}\approx 0.318$
C - Parabolic Flux	$\frac{3}{2}\overline{q}\sqrt{1-(r/a)^2}$	$\frac{9}{32}\approx 0.281$	$\frac{3}{8}\approx 0.375$

Table 2 Effect of shape on isoflux stationary heat sources [11]

R^*	Circular	Square
$\overline{R}ka$	0.270	0.237
$\hat{R}ka$	0.318	0.282

Table 2 presents a comparison of the dimensionless thermal resistance for a circular and square heat source with uniformly distributed heat flux [11]. In both cases, the dimensionless thermal resistance is greater for the circular heat source than for the square source. The relative differences are 12.2 percent for the resistance based upon the average source temperature and 11.3 percent for the resistance based upon the maximum source temperature. Later, it will be shown that if $\mathcal{L}=\sqrt{A}$, the effects of source shape and aspect ratio are minimized. This will eventually lead to a simplified model for an arbitrarily shaped moving heat source.

If the shape of the heat source shown in Figs. 1 and 2 is allowed to vary with aspect ratio $\epsilon=b/a$, then the solutions are somewhat more complex than those given in Table 2. The solution for the dimensionless thermal resistance of a stationary rectangular uniform heat source [11] is

$$\overline{R}ka=\frac{1}{2\pi}\left\{\frac{\sinh^{-1}(\epsilon)}{\epsilon}+\sinh^{-1}(1/\epsilon)+\frac{1}{3}\left[\frac{1}{\epsilon^2}+\epsilon-\frac{(1+\epsilon^2)^{3/2}}{\epsilon^2}\right]\right\} \tag{12}$$

for the average contact temperature, and

$$\hat{R}ka=\frac{1}{2\pi}\left\{\frac{\sinh^{-1}(\epsilon)}{\epsilon}+\sinh^{-1}(1/\epsilon)\right\} \tag{13}$$

for the maximum contact temperature.

The solution for the elliptic heat source was obtained by Yovanovich [5,14–16] and is given by

$$\hat{R}ka=\frac{1}{2\pi}\mathbf{K}(\epsilon') \tag{14}$$

for the isothermal contact, and

$$\overline{R}ka=\frac{16}{3\pi^3}\mathbf{K}(\epsilon') \tag{15}$$

and

$$\hat{R}ka=\frac{2}{\pi^2}\mathbf{K}(\epsilon') \tag{16}$$

for the isoflux contact, where $\epsilon' = \sqrt{1-\epsilon^2}$, and $\mathbf{K}(\epsilon')$ is the complete elliptic integral of the first kind of complementary modulus ϵ'. Equations (15) and (16) were obtained by comparing the limiting case of the circular contact from Table 1 with the result for the isothermal contact. Equations (15) and (16) accurately predict the numerical results presented in [16] for the elliptic contact which were obtained using the method of superposition of point heat sources. No solution was available for the parabolic flux distribution. A solution for this configuration is easily obtained by analogy with the elastic contact problem [20], or by comparison with the solutions presented above. The effect of aspect ratio on a stationary elliptic heat source is

$$f(\epsilon) = \frac{2}{\pi}\mathbf{K}(\epsilon') \tag{17}$$

Thus the solution for the parabolic heat flux distribution is the function $f(\epsilon)$ multiplied by the values for the resistance for Case C in Table 1:

$$\overline{R}ka = \frac{9}{16\pi}\mathbf{K}(\epsilon') \tag{18}$$

and

$$\hat{R}ka = \frac{3}{4\pi}\mathbf{K}(\epsilon'). \tag{19}$$

Equation (19) may also be derived from the analogous elastic contact problem discussed in [20], for the Hertzian pressure distribution.

Moving Heat Sources (Pe$\rightarrow\infty$). Solutions for moving heat sources have been obtained for a number of configurations and boundary conditions. All of the moving source solutions are written in terms of the Peclet number. The Peclet number is defined as

$$\mathrm{Pe} = \frac{V\mathcal{L}}{\alpha}, \tag{20}$$

where $\mathcal{L}$ is a characteristic length scale representative of the contact geometry. If the contact geometry is circular or square then $\mathcal{L}=a$, the radius of the contact or the half side length of the square. Later, it will be shown that if $\mathcal{L}=\sqrt{A}$, the area of the heat source, the effect of shape and aspect ratio on the dimensionless resistance is small.

The effect of heat flux distribution (uniform or parabolic) on the thermal resistance for a moving circular heat source is given in Table 3. The solution for the uniform heat flux distribution was obtained by Archard [17] and the solution for the parabolic heat flux distribution was obtained by Francis [18]. These solutions are only valid for large values of the Peclet number. The effect of flux distribution on the thermal resistance based upon the average contact temperature is small. The relative difference being only 1.6 percent. The relative difference increases to 15.9 percent for the thermal resistance based upon the maximum source temperature.

Table 3 Effect of boundary condition on a moving circular heat source [17,18]

R*	Uniform Flux	Parabolic Flux
$\overline{R}ka$	$\frac{0.318}{\sqrt{Pe}}$	$\frac{0.323}{\sqrt{Pe}}$
$\hat{R}ka$	$\frac{0.508}{\sqrt{Pe}}$	$\frac{0.589}{\sqrt{Pe}}$

Table 4 Effect of shape on isoflux moving heat sources [12,17]

R*	Circular	Square
$\overline{R}ka$	$\frac{0.318}{\sqrt{Pe}}$	$\frac{0.266}{\sqrt{Pe}}$
$\hat{R}ka$	$\frac{0.508}{\sqrt{Pe}}$	$\frac{0.399}{\sqrt{Pe}}$

Finally, Table 4 presents a comparison of the asymptotic solutions for the fast moving heat source for the circular and square heat sources. The results are 16.4 percent and 21.5 percent higher for the circular heat source for the thermal resistance based upon the average and maximum source temperatures, respectively.

If the contact is rectangular the thermal resistance will vary with aspect ratio $\epsilon = b/a$, where $0 < \epsilon < \infty$. The solution obtained by Jaeger [12] for the strip source is applicable to a rectangular heat source since the solution assumes one dimensional heat flow into the half space, i.e., the penetration depth is small compared with the characteristic dimension of the contact zone. The solution for the finite rectangular source [12] is

$$\overline{R}ka = \frac{\sqrt{2}}{3\sqrt{\pi}}\left(\frac{a}{b}\right)\frac{1}{\sqrt{\mathrm{Pe}}} \tag{21}$$

for the average contact temperature, and

$$\hat{R}ka = \frac{\sqrt{2}}{2\sqrt{\pi}}\left(\frac{a}{b}\right)\frac{1}{\sqrt{\mathrm{Pe}}} \tag{22}$$

for the maximum contact temperature, where $\mathrm{Pe} = Va/\alpha$, is based upon the half width of the rectangle in the direction of motion, see Fig. 1.

No solution was found for the fast moving elliptical contact. In order to obtain a solution for the elliptical contact, the approach developed by Jaeger [12] for the square source and by Archard [17] for the circular contact was applied. In this case the effective contact time is

$$t = \frac{2x'}{V} = \frac{2\sqrt{a^2\left(1-\dfrac{y^2}{b^2}\right)}}{V}. \tag{23}$$

Applying the approach of Jaeger [12] and Archard [17] gives

$$\overline{R}ka = \frac{1}{\pi}\left(\frac{a}{b}\right)\frac{1}{\sqrt{\mathrm{Pe}}} \tag{24}$$

for the dimensionless thermal resistance based upon the average contact temperature, and

$$\hat{R}ka = \frac{2\sqrt{2}}{\pi^{3/2}}\left(\frac{a}{b}\right)\frac{1}{\sqrt{\mathrm{Pe}}} \tag{25}$$

for the dimensionless thermal resistance based upon the maximum contact temperature. In both cases, $\mathrm{Pe} = Va/\alpha$ is based upon the half width of the heat source in the direction of motion, see Fig. 2.

Comparison of Eqs. (21) and (22) and Eqs. (24) and (25) with the solutions for the square and circular heat source provided in Table 4, shows that the solutions are identical except for the term (a/b). This factor accounts for the effect of heat source aspect ratio with respect to the direction of motion. These results may be applied to infer the following solutions for a fast moving elliptic heat source with parabolic heat flux distribution:

$$\overline{R}ka = 0.323\left(\frac{a}{b}\right)\frac{1}{\sqrt{\mathrm{Pe}}} \tag{26}$$

and

$$\hat{R}ka = 0.589\left(\frac{a}{b}\right)\frac{1}{\sqrt{\mathrm{Pe}}}. \tag{27}$$

In the next section, the results will applied to develop new models applicable to a real contacts of non-circular shape.

Analysis of Real Contacts

In this section, application of the theory of moving heat sources to real contacts is discussed. A simple approach to modelling the effects of shape, aspect ratio, orientation, and heat flux distribution is presented. It will be assumed that the shape of a real contact is elliptic, and that classic Hertzian analysis for elastic contact of non-conforming surfaces may be used to predict the contact zone dimensions [21].

Effect of Contact Shape. Hertzian theory may be used to predict the contact size for elastic contact. However, this assumes the shape of the contact is elliptic. Depending on the surface topography, this assumption may not be valid. Thus, it is desirable to examine the effect that shape and aspect ratio have on the overall resistance of moving heat sources.

Yovanovich et al. [16] examined the effect of the shape and aspect ratio of an isolated stationary contact having a uniform flux distribution. The geometry examined by Yovanovich et al. [16] was the hyperellipse, defined as

$$\left(\frac{x}{a}\right)^{\gamma} + \left(\frac{y}{b}\right)^{\gamma} = 1, \tag{28}$$

where a and b are the semi-major and semi-minor axis lengths, respectively. The parameter γ determines the shape of the contact. The values of the parameter γ which were examined by Yovanovich et al. [16] were $\gamma=1/2$, $\gamma=1$, and $\gamma=2$. If $\gamma\to\infty$ the hyperellipse becomes a rectangular contact. Yovanovich et al. [16] showed that if the thermal resistance is non-dimensionalized using the square root of the contact area, the solutions are weak functions of shape and aspect ratio.

Table 5 presents the dimensionless resistance based upon the average and centroidal values of temperature for different values of the parameter γ, Yovanovich et al. [16]. It is clearly seen that the dimensionless resistance varies very little with aspect ratio $\epsilon=b/a$ and shape parameter γ. The solutions for the isoflux stationary elliptic heat source become

$$\overline{R}_s k\sqrt{A} = \frac{16}{3\pi^3}\sqrt{\pi\epsilon_s}\mathbf{K}(\epsilon_s') \tag{29}$$

for the average contact temperature, and

$$\hat{R}_s k\sqrt{A} = \frac{2}{\pi^2}\sqrt{\pi\epsilon_s}\mathbf{K}(\epsilon_s') \tag{30}$$

for the maximum contact temperature. If the flux distribution is parabolic, then the solutions presented earlier become

$$\overline{R}_s k\sqrt{A} = \frac{9}{16\pi}\sqrt{\pi\epsilon_s}\mathbf{K}(\epsilon_s') \tag{31}$$

and

$$\hat{R}_s k\sqrt{A} = \frac{3}{4\pi}\sqrt{\pi\epsilon_s}\mathbf{K}(\epsilon_s'). \tag{32}$$

If the heat source is rectangular, then the dimensionless thermal resistance, Eqs. (12, 13) become

Table 5 Dimensionless resistance for stationary isoflux hyperelliptic contacts [16]

	$\gamma = 1/2$		$\gamma = 1$	
ϵ	$\overline{\mathbf{R}}\mathbf{k}\sqrt{\mathbf{A}}$	$\hat{\mathbf{R}}\mathbf{k}\sqrt{\mathbf{A}}$	$\overline{\mathbf{R}}\mathbf{k}\sqrt{\mathbf{A}}$	$\hat{\mathbf{R}}\mathbf{k}\sqrt{\mathbf{A}}$
1.0	0.4440	0.5468	0.4728	0.5611
0.8	0.4428	0.5458	0.4713	0.5597
0.6	0.4376	0.5420	0.4651	0.5540
0.4	0.4237	0.5310	0.4487	0.5385
0.2	0.3860	0.5005	0.4052	0.4957
	$\gamma = 2$		$\gamma = \infty$	
ϵ	$\overline{\mathbf{R}}\mathbf{k}\sqrt{\mathbf{A}}$	$\hat{\mathbf{R}}\mathbf{k}\sqrt{\mathbf{A}}$	$\overline{\mathbf{R}}\mathbf{k}\sqrt{\mathbf{A}}$	$\hat{\mathbf{R}}\mathbf{k}\sqrt{\mathbf{A}}$
1.0	0.4787	0.5642	0.4732	0.5611
0.8	0.4772	0.5624	0.4718	0.5590
0.6	0.4711	0.5551	0.4658	0.5503
0.4	0.4548	0.5360	0.4502	0.5279
0.2	0.4112	0.4845	0.4082	0.4706

$$\overline{R}_s k\sqrt{A} = \frac{\sqrt{\epsilon_s}}{\pi}\left\{\frac{\sinh^{-1}(\epsilon_s)}{\epsilon_s} + \sinh^{-1}(1/\epsilon_s) + \frac{1}{3}\left[\frac{1}{\epsilon_s^2} + \epsilon_s - \frac{(1+\epsilon_s^2)^{3/2}}{\epsilon_s^2}\right]\right\} \tag{33}$$

for the average contact temperature, and

$$\hat{R}_s k\sqrt{A} = \frac{\sqrt{\epsilon_s}}{\pi}\left\{\frac{\sinh^{-1}(\epsilon_s)}{\epsilon_s} + \sinh^{-1}(1/\epsilon_s)\right\} \tag{34}$$

for the maximum contact temperature. Since the effect of aspect ratio is small, average values of the dimensionless resistance given in Table 5 may be used to approximate the resistance for a heat source with variable aspect ratio.

In the case of the moving heat source the Peclet number should also be based upon the square root of the contact area, i.e., $\mathcal{L} = \sqrt{A}$ in Eq. (20). Table 6 summarizes the results for the rectangular and elliptic heat sources for different heat flux distributions, when the resistance is non-dimensionalized using the square root

Table 6 Dimensionless resistance of moving heat sources on a half-space

Shape (Boundary condition)	$\overline{\mathbf{R}}\mathbf{k}\sqrt{\mathbf{A}}$	$\hat{\mathbf{R}}\mathbf{k}\sqrt{\mathbf{A}}$
Rectangular (Isoflux)	$\dfrac{0.752}{\sqrt{Pe^*_{\sqrt{A}}}}$	$\dfrac{1.130}{\sqrt{Pe^*_{\sqrt{A}}}}$
Elliptic (Isoflux)	$\dfrac{0.750}{\sqrt{Pe^*_{\sqrt{A}}}}$	$\dfrac{1.200}{\sqrt{Pe^*_{\sqrt{A}}}}$
Elliptic (Parabolic Flux)	$\dfrac{0.762}{\sqrt{Pe^*_{\sqrt{A}}}}$	$\dfrac{1.390}{\sqrt{Pe^*_{\sqrt{A}}}}$

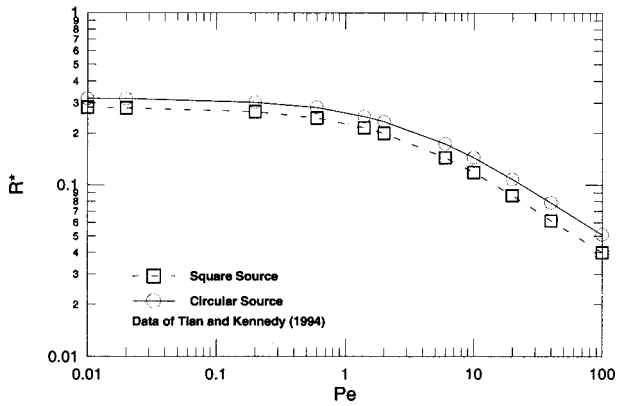

Fig. 3 $\hat{R}_a^*$ **versus** Pe_a **for a circular and square moving heat source**

of the contact area. Comparisons of the dimensionless resistance $\hat{R}^*$ are provided in Figs. 3 and 4 using the data for the exact analytical solutions of a isoflux heat sources from Tian and Kennedy [8]. Figure 3 shows a comparison of the results for a circular and square heat source when the characteristic length is $\mathcal{L}=a$. In Figure 4, the results for each geometry have virtually collapsed onto one another when $\mathcal{L}=\sqrt{A}$. Thus the effect of the shape of the heat source is not a significant factor, when the results are appropriately non-dimensionalized.

If the heat source is rectangular or elliptical the Peclet number must be replaced with a modified Peclet number Pe* defined as

$$\mathrm{Pe}^*_{\sqrt{A}}=(\epsilon_m)^{1/2}\mathrm{Pe}_{\sqrt{A}}. \tag{35}$$

The aspect ratio $\epsilon_m=b/a$ now accounts for the effect of the shape and orientation of the heat source. Since a rectangular or elliptic heat source may be oriented in the direction of motion parallel to the short or long axis of the heat source, the resistance must change based on orientation. Given the same source area and velocity, the Peclet number remains unchanged, but the resistance will decrease if the direction of motion is parallel to the short axis of the heat source. Thus, for a moving heat source, $0<\epsilon_m<\infty$. This is quite important for the moving heat source since the resistance will increase with decreasing ϵ_m, i.e., $a>b$, and decrease with increasing ϵ_m, i.e., $b>a$. If the heat source is stationary, the orientation of the contact is not important and $0<\epsilon_s<1$.

Models for $0<\mathrm{Pe}<\infty$. In the previous sections the thermal resistances of isolated stationary and fast moving contacts were presented. These solutions represent asymptotic solutions for large and small values of the Peclet number. If the contact is moving at moderate speeds $0.1<\mathrm{Pe}<10$, a composite solution is required. Tian and Kennedy [8] combined the asymptotic results for the circular heat source using an equation which is a special case of the more general form

$$\frac{1}{R_t^n}=\frac{1}{R_s^n}+\frac{1}{R_m^n}. \tag{36}$$

Equation (36) is one form of the asymptotic correlation method proposed by Churchill and Usagi [22]. This method allows the combination of asymptotic solutions, to generate a model which is valid for all values of the dependent parameter.

A single value of $n=2$ was found to give excellent agreement between the approximate model and numerical results of Tian and Kennedy [8] over the entire range of Peclet numbers for the circular heat source having a uniform or parabolic heat flux distribution and a square heat source having a uniform heat flux distribution. Thus, the parameter n does not appear to depend upon the shape of the source or the flux distribution. The models developed by Tian and Kennedy [8] are specifically for the circular heat source for uniform and parabolic flux distributions. They are not applicable to elongated contacts such as elliptic or rectangular contacts. In addition, Tian and Kennedy [8] presented their correlations in terms of contact temperatures; rather than thermal resistance. The use of thermal resistance facilitates the calculation of the partition of heat into the contacting bodies.

A general model for a moving heat source will now be obtained by combining the dimensionless resistances for a stationary and fast moving heat sources in the form of Eq. (36). As noted earlier, the definition of aspect ratio is different for the moving and stationary heat sources. The aspect ratio of the stationary heat source is now denoted by $\epsilon_s=b/a$ such that $0<\epsilon_s<1$, and the aspect ratio of the moving heat source is now denoted by ϵ_m such that $0<\epsilon_m<\infty$. Also, since the effect of shape has been shown to be negligible, only the solution for the elliptic heat source will be considered in the model development.

Combining the stationary and moving heat source solutions for both the average and maximum contact surface temperatures gives

$$\overline{R}_t k\sqrt{A}=\frac{0.750}{\sqrt{(\epsilon_m)^{1/2}\mathrm{Pe}_{\sqrt{A}}+6.05/(\epsilon_s\mathbf{K}^2(\epsilon_s'))}} \tag{37}$$

and

$$\hat{R}_t k\sqrt{A}=\frac{1.200}{\sqrt{(\epsilon_m)^{1/2}\mathrm{Pe}_{\sqrt{A}}+11.16/(\epsilon_s\mathbf{K}^2(\epsilon_s'))}} \tag{38}$$

for the uniform flux distribution, and

$$\overline{R}_t k\sqrt{A}=\frac{0.762}{\sqrt{(\epsilon_m)^{1/2}\mathrm{Pe}_{\sqrt{A}}+5.77/(\epsilon_s\mathbf{K}^2(\epsilon_s'))}} \tag{39}$$

and

$$\hat{R}_t k\sqrt{A}=\frac{1.390}{\sqrt{(\epsilon_m)^{1/2}\mathrm{Pe}_{\sqrt{A}}+10.79/(\epsilon_s\mathbf{K}^2(\epsilon_s'))}} \tag{40}$$

for the parabolic flux distribution. These expressions can now be applied to arbitrarily shaped heat sources for all values of the Peclet number.

Bounds on Thermal Resistance. The expressions developed previously for the elliptic heat source assume that it is oriented with one of the axes parallel to the direction of motion, see Fig. 2. Equations (37–40) are not valid for a heat source oriented at an angle to the direction of motion. The solution for this case requires integration over the surfaces of the oblique orientation. However, Eqs. (37–40) may be used to bound the values by considering the results for the two extreme cases of ϵ_m. The limiting

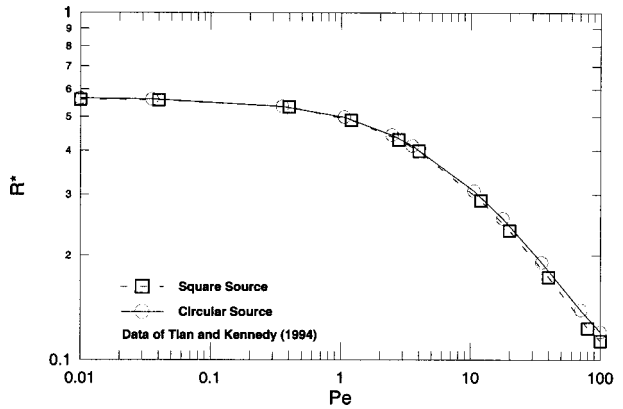

Fig. 4 $\hat{R}^*_{\sqrt{A}}$ **versus** $\mathrm{Pe}_{\sqrt{A}}$ **for a circular and square moving heat source**

cases may then be averaged in a number of ways. It is proposed that the bounding values be weighted using following expression

$$R^* = R_x^* \cos^2(\theta) + R_y^* \sin^2(\theta), \tag{41}$$

where R_x^* denotes the dimensionless resistance based upon the aspect ratio in the x-direction, and R_y^* denotes the dimensionless resistance based upon the aspect ratio in the y-direction. This formulation is proposed since it reduces to the limiting cases for $\theta = 0$ deg and $\theta = 90$ deg, and returns the arithmetic average at $\theta = 45$ deg. In the absence of an exact solution, Eq. (41) should provide good results for the average or maximum temperature prediction.

Prediction of Flash Temperatures. The concept of maximum or average flash temperature is discussed in detail in Archard [17], Blok [23], Winer and Cheng [3], and Cowan and Winer [4]. The computation of the flash temperature assumes that one of the contacting surfaces is a stationary heat source and the other a moving heat source. By accounting for the partition of heat into each of the surfaces, an estimate for the average or maximum temperature may be obtained.

In the previous section a general model for an isolated moving source for $0 < \mathrm{Pe} < \infty$ was developed. This model may now be used to predict the average or maximum flash temperatures. The analysis begins by defining the total heat flow and the partition of each into the two contacting surfaces. The total heat generated by sliding friction is denoted $Q_g = \mu FV$, where μ is the coefficient of friction, while the heat which flows into the stationary and moving surfaces are denoted Q_s and Q_m, respectively. Through conservation of energy, the total heat flow is then

$$Q_g = Q_s + Q_m, \tag{42}$$

which may be written in terms of the temperature excess and resistance in each surface

$$\mu FV = \frac{(T_s - T_{b,s})}{R_s} + \frac{(T_m - T_{b,m})}{R_m}. \tag{43}$$

Now if perfect thermal contact is assumed at the interface, then $T_s = T_m = T_c$ at all points within the contact, and the expression given above may be solved for T_c

$$T_c = \frac{\mu FV + \dfrac{T_{b,s}}{R_s} + \dfrac{T_{b,m}}{R_m}}{\dfrac{1}{R_s} + \dfrac{1}{R_m}}. \tag{44}$$

The general expression given above may be applied to any combination of slow, moderate or fast moving sources using the expressions developed earlier. If the bulk temperatures are equal, Eq. (44) may be further simplified. In the case of a typical sliding asperity contact, the system is modelled as a stationary heat source and a moving heat source in parallel. Equation (44) may be written in terms of the dimensionless thermal resistance $R^* = Rk\sqrt{A}$ to give

$$T_c = \frac{\mu FV + \dfrac{T_{b,s}\sqrt{A}k_s}{R_s^*} + \dfrac{T_{b,m}\sqrt{A}k_m}{R_m^*}}{\dfrac{\sqrt{A}k_s}{R_s^*} + \dfrac{\sqrt{A}k_m}{R_m^*}}, \tag{45}$$

which may be further simplified to give

$$T_c = \frac{(\mu FVR_s^*R_m^*)/\sqrt{A} + T_{b,s}k_sR_m^* + T_{b,m}k_mR_s^*}{k_sR_m^* + k_mR_s^*}, \tag{46}$$

where the value for R_s^* is taken to be the appropriate value of the stationary dimensionless resistance Eqs. (29–32) and R_m^* is the appropriate expression for the dimensionless resistance of a moving heat source Eqs. (37–40) which were presented in the previous section. Thus, T_c may be computed for either the maximum or average value which occurs within the contact for either the isoflux or parabolic flux distribution. The validity of Eq. (46) may be questioned on the grounds that the temperature distribution of the real contact will be skewed, however, models for the stationary heat source resistance assume a symmetric temperature profile. For a slow moving contact $\mathrm{Pe} < 0.1$ the profile is nearly symmetric and the partition of heat into each of the surfaces is equal assuming that each surface has the same thermal properties. For a fast moving heat source $\mathrm{Pe} > 10$, the maximum temperature is located at or near the trailing edge. Most of the heat will be conducted into the moving surface since it has a lower thermal resistance. In the transition region $0.1 < \mathrm{Pe} < 10$, the effect of temperature distribution shape should be small since the maximum temperature is located between the centroid and the trailing edge. Thus, Eq. (46) may be applied for either the average or maximum contact temperature basis. Also, due to the relatively short contact times and size of asperities, the penetration depth will be small and the assumption of a half-space is then reasonable.

Table 7 Comparison of average flash temperature results [12]

		Eq. (46)		[12]	
V m/s	Pe	$\overline{T_c}$, °C	$\beta = \frac{Q_m}{Q_g}$	$\overline{T_c}$, °C	$\beta = \frac{Q_m}{Q_g}$
15	16.95	1399.7	0.740	1370	0.74
10	11.30	1057.2	0.705	1040	0.70
7	7.91	816.3	0.675	810	0.67
5	5.65	632.9	0.647	630	0.64
2	2.26	299.5	0.582	300	0.58
1	1.13	161.9	0.548	160	0.54
0.7	0.79	116.5	0.536	115	0.53
0.5	0.57	84.9	0.526	85	0.52
0.2	0.23	35.0	0.517	35	0.51

Table 7 presents a comparison of results computed by Jaeger [12] for mild steel $k = 60.3$ W/mK, $\alpha = 17.7 \times 10^{-6}$ m^2/s, $F = 400$ g, and $\mu = 0.23$ for a square source with half side length $a = 1 \times 10^{-5}$ m. The maximum difference between the model and the data of Jaeger [12] is 2.1 percent at $V = 15$ m/s. This error is small considering that the values presented by Jaeger [12] were based upon graphical results which are also subject to round off errors.

In the final example, the proposed model is compared with numerical results reported by Neder et al. [9]. The system examined by Neder et al. [9] consisted of a bronze substrate ($\alpha = 13.8 \times 10^{-6}$ m^2/s, $k = 50$ W/mK) and a steel slider ($\alpha = 20.0 \times 10^{-6}$ m^2/s, $k = 62$ W/mK). The maximum pressure considered was $P = 450$ MPa and the coefficient of friction $\mu = 0.25$. Neder et al. [9] considered sliding in directions perpendicular and parallel to the grinding direction of a real surface. Some difficulty was encountered interpreting the data reported by Neder et al. [9]. The authors reported a range for the equivalent diameter of the largest real contact spot in the direction parallel and perpendicular to the direction of sliding along with the contact width, $2a$, in the sliding direction only. The equivalent diameters which were tabulated by Neder et al. [9] have different values for each direction. It is assumed that if the same surface was considered, the equivalent diameter should be the same in both sliding directions, and that the contact spot aspect ratio may be computed assuming an elliptic contact. The area is given by $A = \pi D_e^2/4 = \pi ab$. Given D_e and $2a$, $2b$ is computed using ($8\ \mu\mathrm{m} < D_e < 10\ \mu\mathrm{m}$) and ($6\ \mu\mathrm{m} < 2a < 8\ \mu\mathrm{m}$). These dimensions were examined for both sliding directions and the maximum flash temperatures were computed

Table 8 Comparison of maximum flash temperature results [9]

V	D_e	$2a$	$2b$	Eq. (46)	$\hat{T}$
m/s	μm	μm	μm	$°C$	$°C$
1	8-10	6-8	10.7-12.5	3.83-4.81	4.33
1	8-10	10.7-12.5	6-8	3.87-4.86	5.06
10	8-10	6-8	10.7-12.5	32.01-39.17	35.4
10	8-10	10.7-12.5	6-8	34.57-41.98	40.5

using Eq. (54) along with the expressions for the dimensionless resistance based upon the maximum contact temperature. Results are summarized in Table 8. The predicted temperature range is in excellent agreement with the reported values given by Neder et al. [9]. Neder et al. [9] also reported values of $\hat{T}=32.8°C$ and $\hat{T}=37.5°C$ on two plots for the $V=10$ m/s case, in the direction perpendicular and parallel to the grinding direction, respectively. These results are also within the range of temperatures computed using the proposed model.

Summary and Conclusions

A review of the important literature for stationary and moving heat sources was presented. The effects of shape and heat flux distribution for elliptic and rectangular heat sources were examined. It was shown that the dimensionless thermal resistance is a weak function of shape for stationary and moving heat sources when the results are non-dimensionalized using the square root of the heat source area. A simple model for all values of the Peclet number was developed by combining the asymptotic solutions for stationary and moving heat sources. A method was proposed for predicting the thermal resistance of an elliptic heat source oriented at any angle with respect to the direction of motion. These results were then applied to develop a general expression for determining the flash temperature for real surfaces in sliding contact. The proposed model was compared with recent numerical data for real contacts of non-circular shape. Excellent agreement between the model and data was obtained for both elliptic and square contacts.

Acknowledgments

The authors acknowledge the financial support of the Natural Sciences and Engineering Research Council of Canada under operating grant A7455. The first author would also like to thank Dr. J.B. Medley of the Department of Mechanical Engineering, University of Waterloo.

Nomenclature

a = semi-major axis of ellipse or rectangle, radius of circle, m
A = area, m^2
b = semi-minor axis of ellipse or rectangle, m
$\mathbf{E}(\cdot)$ = complete elliptic integral of the second kind
F = applied load, N
k = thermal conductivity, W/mK
$\mathbf{K}(\cdot)$ = complete elliptic integral of the first kind
$\mathcal{L}$ = arbitrary length scale, m
P = pressure, MPa
$\mathrm{Pe}_{\mathcal{L}}$ = Peclet number, $\equiv V\mathcal{L}/\alpha$
$\mathrm{Pe}^*_{\mathcal{L}}$ = modified Peclet number, $\equiv\sqrt{\epsilon}\mathrm{Pe}$
q = heat flux, W/m^2
$\overline{q}$ = average heat flux, $\equiv Q/A$
Q = heat flow rate, W
R = thermal resistance, K/W
R^* = dimensionless thermal resistance, $\equiv Rk\mathcal{L}$
t = time, s
T = temperature, K
T_b = bulk temperature, K
T_c = contact temperature, K
V = velocity, m/s

Greek Symbols

α = thermal diffusivity, m^2/s
δ = thermal penetration depth, m
ϵ = ellipticity or aspect ratio, $\equiv b/a$
ϵ' = complementary modulus, $\equiv\sqrt{1-\epsilon^2}$
ϵ_m = aspect ratio, moving source, $0<b/a<\infty$
ϵ_s = aspect ratio, stationary source, $0<b/a<1$
ϕ = angle between principal planes of contact, rad
γ = hyperellipse parameter
θ = temperature excess, K
μ = coefficient of friction
ν = Poisson's ratio
θ = angle, rad

Superscripts

$\overline{(\cdot)}$ = based on the average temperature
$\widehat{(\cdot)}$ = based on maximum temperature

Subscripts

1,2 = surface 1, surface 2
$\sqrt{A}$ = based on $\mathcal{L}=\sqrt{A}$
b = bulk
c = contact
g = generated
$\mathcal{L}$ = arbitrary length scale $\mathcal{L}$
m = moving
s = stationary
t = total

References

[1] Halling, J., 1975, *Principles of Tribology*, MacMillan Education Ltd.
[2] Williams, J. A., 1994, *Engineering Tribology*, Oxford University Press.
[3] Winer, W. O., and Cheng, H. S., 1980, ''Film Thickness, Contact Stress and Surface Temperatures,'' in *Wear Control Handbook*, ASME Press, New York, pp. 81–141.
[4] Cowan, R. S., and Winer, W. O., 1992, ''Frictional Heating Calculations,'' in *ASM Handbook, Volume 18 Friction, Lubrication, and Wear Technology*, ASM International, pp. 39–44.
[5] Yovanovich, M. M., 1971, ''Thermal Constriction Resistance Between Contacting Metallic Paraboloids: Application to Instrument Bearings,'' *AIAA Progress in Astronautics and Aeronautics: Heat Transfer and Spacecraft Control, 24*, J. W. Lucas, ed., MIT Press, pp. 337–358.
[6] Yovanovich, M. M., 1978, ''Simplified Explicit Elastoconstriction Resistance Expression for Ball/Race Contacts,'' AIAA Paper 78–84.
[7] Bejan, A., 1989, ''Theory of Rolling Contact Heat Transfer,'' ASME J. Heat Transfer, **111**, pp. 257–263.
[8] Tian, X., and Kennedy, F. E., 1994, ''Maximum and Average Flash Temperatures in Sliding Contacts,'' ASME J. Tribol. **116**, pp. 167–174.
[9] Neder, Z., Varadi, K., Man, L., and Friedrich, K., 1998, ''Numerical and Finite Element Contact Temperature Analysis of Steel-Bronze Real Surfaces in Dry Sliding Contact,'' *ASME/STLE Tribology Conference*, Toronto, Canada.
[10] Cameron, A., Gordon, A. N., and Symm, G. T., 1968, ''Contact Temperatures in Rolling/Sliding Surfaces,'' Proc. R. Soc., London, Ser. A **A268**, pp. 45–61.
[11] Carslaw, H. S., and Jaeger, J. C., 1959, *Conduction of Heat in Solids*, Oxford University Press.
[12] Jaeger, J. C., 1942, ''Moving Sources of Heat and Temperature at Sliding Contacts,'' Proceedings of the Royal Society, New South Wales, **76**, pp. 203–224.
[13] Rosenthal, D., 1946, ''The Theory of Moving Sources of Heat and Its Application to Metal Treatments,'' Trans. ASME, **68**, pp. 849–866.
[14] Yovanovich, M. M., 1988, ''Chapter 8: Theory and Applications of Constriction and Spreading Resistance Concepts for Microelectronic Thermal Management,'' in *Advances in Cooling Techniques for Computers*, Hemisphere Publishing.
[15] Yovanovich, M. M., 1998, ''Chapter 3: Conduction and Thermal Contact Resistance (Conductance),'' in *Handbook of Heat Transfer*, W. M. Rohsenow, J. P. Hartnett, and Y. L. Cho, eds., McGraw-Hill, New York.
[16] Yovanovich, M. M., Burde, S. S., and Thompson, J. C., 1977, ''Thermal Constriction Resistance of Arbitrary Planar Contacts with Constant Heat Flux,'' *AIAA Progress in Astronautics and Aeronautics: Thermophysics of Spacecraft and Outer Planet Entry Probes*, **56**, A. M. Smith, ed., pp. 127–139.
[17] Archard, J. F., 1958, ''The Temperature of Rubbing Surfaces,'' Wear, **2**, pp. 438–455.

[18] Francis, H. A., 1970, ''Interfacial Temperature Distribution Within a Sliding Hertzian Contact,'' ASLE Trans., **14**, pp. 41–54.
[19] Holm, R., 1968, *Electric Contacts*, Springer-Verlag.
[20] Johnson, K. L., 1985, *Contact Mechanics*, Cambridge University Press.
[21] Yovanovich, M. M., 1986, ''Recent Developments in Thermal Contact, Gap, and Joint Conductance Theories and Experiment,'' *Heat Transfer 1986, Proceedings of the Eighth International Heat Transfer Conference*, **1**, pp. 35–45.
[22] Churchill, S. W., and Usgai, R., 1972, ''A General Expression for the Correlation of Rates of Transfer and Other Phenomena,'' American Institute of Chemical Engineers, **18**, pp. 1121–1128.
[23] Blok, H., 1963, ''The Flash Temperature Concept,'' Wear, **6**, pp. 483–494.